XLIII CILAMCE
21–25, November, 2022
FOZ DO IGUAÇU – PR – BRAZIL

Computational modelling of tendons: poromechanical approach for micro-scales

Bruno Klahr[1], José L. M. Thiesen[1], Otávio T. Pinto[1], Thiago A. Carniel[2], Eduardo A. Fancello[1]

[1]*Dept. of Mechanical Engineering, Federal University of Santa Catarina*
Florianópolis, 88040-900, Santa Catarina, Brazil
bruno.klahr@posgrad.ufsc.br, jose.thiesen@posgrad.ufsc.br,otavio.pinto@posgrad.ufsc.br, eduardo.fancello@ufsc.br
[2]*Polytechical School, Community University of Chapecó Region*
Chapecó, 89809-900, Santa Catarina, Brazil
thiago.carniel@unochapeco.edu.br

Abstract. Fluid flow effects on the microstructure of soft biological tissues are of fundamental importance in understanding mechanobiological processes, such as in mechanotransduction. Since these tissues are highly heterogeneous and have a large microstructural hierarchy, investigations of macroscopic behavior by incorporating microstructural effects can be performed using multiscale techniques. This work aims to bring additional discussion related to the micromechanics of fibrous biological tissues such as tendons. For this purpose, technical aspects involving the first-order multiscale formulation developed by the authors are discussed, presenting advantages and limitations of this type of model. Some results related to a multiscale framework that considers hydro-mechanical coupling are presented and discussed, aiming point out some features of the formulation.

Keywords: Computational modelling, tendon mechanics, micromechanics, poromechanics.

1 Introduction

While in healthy conditions tendons play the functional role of providing mechanical continuity between bones and muscles, their malfunction is capable of seriously compromising motor skills and quality of life. Studies in the literature about their mechanical modeling are mostly related to macroscopic biomechanical function, leading to phenomenological constitutive expressions whose complexity is chosen according to the specific application. Less (but increasingly) frequently, one finds models whose focus is on the structural complexity of the tissue itself, with the aim of understanding the mechanical role in tissue homeostasis and in triggering pathological processes.

In the latter case, a close look at the tissue will show a highly hierarchical multi-scale complex structure comprising subtendons, fascicles, cells, fibrils, collagen molecules, and other components. As a consequence, a simple macro-scale uniaxial stress state branches out into a complex heterogeneous micro-scale stress field.

Being cells the protagonist of mechano-transduction activity, the fascicle scale (cells and fibers in a geometric arrangement), is of particular interest [1–3]. At such a scale, the intrinsic dissipative properties of the solid phase as well as the fluid flow process play an important role. Poromechanical models, largely used in biological macroscopic systems like intervertebral disks and cartilaginous joints, re-emerge as a valid modeling framework for tendons at such scale where multiscale/homogenization theories bring suitable alternatives for analysis. In recent years, some authors have addressed appropriate homogenization frameworks for multiphase models [4–6], but less information is recovered when large deformations take place.

In this context, a proposition of finite-strain multiscale framework considering hydro-mechanical coupling under large deformations is ongoing in the first author's PhD thesis. This formulation is based on the axioms of the Multiscale Virtual Power Method proposed in Blanco et al. [7]. Since this work is grounded in a variational approach, the multiscale boundary conditions are established through the so-called minimally restricted spaces, which constraint the displacement and pore pressure fields. This paper aims to contribute to the investigation and discussion of the proposed multiscale poromechanical model. In this case, further numerical results are discussed in order to pursue the main objective of finding answers to biomechanical/clinical questions in such tissues mechanics.

2 Computational modeling

2.1 Poromechanics formulation

Poromechanical formulations model a porous medium consisting of a fluid flowing through a deformable porous solid, but in a homogenized fashion at the macro-scale level. Thus, such a class of models does not consider an explicit separation between the solid and the fluid phase.

Considering poromechanical models applied to soft tissues, some fundamental assumptions are generally considered. At first, the solid skeleton is considered to be completely saturated with only one fluid phase. Furthermore, the fluid and the solid material are considered to be intrinsically incompressible, although the solid skeleton is considered to be compressible, allowing fluid flow during deformation. Regarding the stress field of the porous medium, the total Cauchy stress tensor is defined by a sum of a fluid contribution, which depends only on the pore pressure, and a solid contribution, which in turn usually depends only on the deformation of the solid skeleton.

The variational form (weak form) of the governing equation of the macro-scale porous domain [8, 9], in the absence of inertial and body forces, can be written in the referential configuration by,

$$\begin{aligned} \delta W^{\mathrm{s}} &= \int_{\Omega_{\mathrm{X}}} \mathbf{P} : \delta\mathbf{F}\, \mathrm{d}\Omega_{\mathrm{X}} - \int_{\partial\Omega_{\mathrm{X}}|_{\mathbf{t}}} \bar{\mathbf{t}}_{\mathrm{X}} \cdot \delta\mathbf{u}\, \mathrm{d}\partial\Omega_{\mathrm{X}} = 0, \qquad \forall\delta\mathbf{u} \in \mathscr{V}_{\mathbf{u}} \qquad \text{and} \\ \delta W^{\mathrm{f}} &= \int_{\Omega_{\mathrm{X}}} \dot{J}\, \delta p\, \mathrm{d}\Omega_{\mathrm{X}} - \int_{\Omega_{\mathrm{X}}} \mathbf{w}_{\mathrm{X}} \cdot \boldsymbol{\nabla}_{\mathrm{X}} \delta p\, \mathrm{d}\Omega_{\mathrm{X}} + \int_{\partial\Omega_{\mathrm{X}}|_{q}} \bar{q}_{\mathrm{X}}\, \delta p\, \mathrm{d}\partial\Omega_{\mathrm{X}} = 0, \qquad \forall\delta p \in \mathscr{V}_{p}, \end{aligned} \tag{1}$$

in which the total first Piola-Kirchhoff stress tensor is given by $\mathbf{P} = J\left(\boldsymbol{\sigma}^{\mathrm{s}} - p\mathbf{I}\right)\mathbf{F}^{-\mathrm{T}}$, where $\boldsymbol{\sigma}^{\mathrm{s}}$ is the solid skeleton Cauchy stress and p is the pore pressure. In this line, $\delta\mathbf{F}{=}\boldsymbol{\nabla}_{\mathrm{X}}\delta\mathbf{u}$ is the first variation of the deformation gradient $\mathbf{F}$. The scalar $J = \det(\mathbf{F})$ is the volumetric jacobian, and its rate is given by $\dot{J} = \mathrm{tr}\left(\boldsymbol{\nabla}_{\mathrm{X}}\mathbf{v}^{\mathrm{s}}\mathbf{F}^{-1}\right)J$, where the operator $\mathrm{tr}(\cdot)$ is the trace operator. The vector $\mathbf{w}_{\mathrm{X}} = J\mathbf{F}^{-1}\mathbf{w}$ represents the referential relative velocity and the operator $\boldsymbol{\nabla}_{\mathrm{X}}(\cdot)$ is the referential gradient operator. The vector $\bar{\mathbf{t}}_{\mathrm{X}}$ and the scalar $\bar{q}_{\mathrm{X}}$ are the referential external surface traction and the referential external surface flux, respectively. Moreover, $\mathscr{V}_{\mathbf{u}}$ and $\mathscr{V}_{p}$ represent the macro-scale referential admissible spaces for the variations $\delta\mathbf{u}$ and δp, respectively. The poromechanical formulation and coupled solution methods used in this work are extensively presented in Klahr et al. [10].

2.2 Computational homogenization poromechanical model

Considering the poromechanical modeling, the primary modeling variables are the displacement and the pore pressure. Therefore, it is necessary to define the insertion operation for these variables, which in computational homogenization refers to the operation of transferring the quantities from the macro scale to the micro scale.

The micro-scale displacement field $\mathbf{u}_{\mu}(\mathbf{Y}, t)$ can be extended by,

$$\mathbf{u}_{\mu}(\mathbf{Y}, t) = \mathbf{u}(\mathbf{X}, t) + \boldsymbol{\nabla}_{\mathrm{X}}\mathbf{u}(\mathbf{X}, t)\,\mathbf{Y} + \tilde{\mathbf{u}}_{\mu}(\mathbf{Y}, t), \tag{2}$$

where $\mathbf{u}(\mathbf{X}, t)$ and $\boldsymbol{\nabla}_{\mathrm{X}}\mathbf{u}(\mathbf{X}, t)$ are the macro-scale displacement and its referential gradient, respectively, $\mathbf{Y}$ is the micro-scale referential position and $\tilde{\mathbf{u}}_{\mu}$ is the micro-scale displacement fluctuation field. Similarly, the micro-scale pore pressure field $p_{\mu}(\mathbf{Y}, t)$ is expanded as,

$$p_{\mu}(\mathbf{Y}, t) = p(\mathbf{X}, t) + \boldsymbol{\nabla}_{\mathrm{X}}p(\mathbf{X}, t) \cdot \mathbf{Y} + \tilde{p}_{\mu}(\mathbf{Y}, t), \tag{3}$$

where $p(\mathbf{X}, t)$ and $\boldsymbol{\nabla}_{\mathrm{X}}p(\mathbf{X}, t)$ are the macro-scale pore pressure and its referential gradient, respectively, and $\tilde{p}_{\mu}$ is the micro-scale pore pressure fluctuation field.

Defining the concept of volumetric homogenization in the referential setting, which relates the macro-scale quantities to the micro-scale fields, we define the homogenization operator as

$$\langle(\cdot)\rangle = \frac{1}{V_{\mu}} \int_{\Omega_{\mathrm{Y}}} (\cdot)\, \mathrm{d}\Omega_{\mathrm{Y}}, \tag{4}$$

where V_{μ} is the referential volume of the RVE.

This multiscale poromechanical assumes two constraints. Firstly, it is proposed that the homogenization of the micro-scale fields of primaty variables $\mathbf{u}_{\mu}(\mathbf{Y}, t)$ and $p_{\mu}(\mathbf{Y}, t)$ are related to their macro-scale fields, *i.e.*:

$$\langle\mathbf{u}_{\mu}(\mathbf{Y}, t)\rangle = \mathbf{u}(\mathbf{X}, t) \qquad \text{and} \qquad \langle p_{\mu}(\mathbf{Y}, t)\rangle = p(\mathbf{X}, t), \tag{5}$$

Secondly, it is assumed that the volumetric homogenization of the micro-scale gradient fields must be equal to the corresponding macro-scale gradients,

$$\langle \boldsymbol{\nabla}_{\mathrm{Y}} \mathbf{u}_{\mu}(\mathbf{Y},t)\rangle = \boldsymbol{\nabla}_{\mathrm{X}}\mathbf{u}(\mathbf{X},t) \qquad \text{and} \qquad \langle \boldsymbol{\nabla}_{\mathrm{Y}} p_{\mu}(\mathbf{Y},t)\rangle = \boldsymbol{\nabla}_{\mathrm{X}} p(\mathbf{X},t)\,. \tag{6}$$

The energetic consistency between micro and macro-scales was established through the so-called Hill-Mandel Principle of Macro-homogeneity [11, 12]. In this work, we follow the proposition established in [7], where the Hill-Mandel Principle is rewritten in a variational statement. In this case, the Principle of Multiscale Virtual Power proposes that the total macro-scale virtual power must be equal to the total micro-scale virtual power at the corresponding RVE subjected to all kinematically admissible boundary conditions, that is,

$$\mathsf{P}_{\mathrm{M}}^{\text{total}}\left(\delta\dot{\mathbf{F}}, \delta p, \boldsymbol{\nabla}_{\mathrm{X}}\delta p\right) = \mathsf{P}_{\mu}^{\text{total}}\left(\delta\dot{\tilde{\mathbf{u}}}_{\mu}, \delta\tilde{p}_{\mu}\right). \tag{7}$$

Based on the poromechanical formulation presented in Eq. (1), the total macro-scale virtual power is defined as

$$\mathsf{P}_{\mathrm{M}}^{\text{total}}\left(\delta\dot{\mathbf{F}}, \delta p, \boldsymbol{\nabla}_{\mathrm{X}}\delta p\right) = \mathbf{P} : \delta\dot{\mathbf{F}} + \dot{J}\,\delta p - \mathbf{w}_{\mathrm{X}}\cdot\boldsymbol{\nabla}_{\mathrm{X}}\delta p \quad \forall\left(\delta\dot{\mathbf{F}}, \delta p, \boldsymbol{\nabla}_{\mathrm{X}}\delta p\right) \tag{8}$$

and its micro-scale counterpart is written as

$$\mathsf{P}_{\mu}^{\text{total}}\left(\delta\dot{\tilde{\mathbf{u}}}_{\mu}, \delta\tilde{p}_{\mu}\right) = \left\langle \mathbf{P}_{\mu} : \delta\dot{\mathbf{F}}_{\mu} + \dot{J}_{\mu}\,\delta p_{\mu} - \mathbf{w}_{\mathrm{Y}}\cdot\boldsymbol{\nabla}_{\mathrm{Y}}\delta p_{\mu}\right\rangle \quad \forall\left(\delta\dot{\tilde{\mathbf{u}}}_{\mu}, \delta\tilde{p}_{\mu}\right) \in \mathcal{V}_{\tilde{\mathbf{u}}_{\mu}} \times \mathcal{V}_{\tilde{p}_{\mu}}, \tag{9}$$

where $\mathcal{V}_{(\cdot)}$ is the kinematically admissible space referring to variation of the variable $(\cdot)$ in the referential configuration. From the aforementioned principle, the equilibrium (mechanical balance) and mass conservation equations satisfied at the microscale can be derived, providing the following variational expressions on the RVE domain:

$$\int_{\Omega_{\mathrm{Y}}} \mathbf{P}_{\mu} : \boldsymbol{\nabla}_{\mathrm{Y}}\delta\dot{\tilde{\mathbf{u}}}_{\mu}\,\mathrm{d}\Omega_{\mathrm{Y}} = 0, \qquad \forall\delta\dot{\tilde{\mathbf{u}}}_{\mu} \in \mathcal{V}_{\tilde{\mathbf{u}}_{\mu}}, \qquad \text{and} \tag{10}$$

$$\int_{\Omega_{\mathrm{Y}}} \left[\delta\tilde{p}_{\mu}\dot{J}_{\mu} - \boldsymbol{\nabla}_{\mathrm{Y}}\delta\tilde{p}_{\mu}\cdot\mathbf{w}_{\mathrm{Y}}\right]\mathrm{d}\Omega_{\mathrm{Y}} = 0, \qquad \forall\delta\tilde{p}_{\mu} \in \mathcal{V}_{\tilde{p}_{\mu}}. \tag{11}$$

In addition to the equilibrium equations, the homogenizations of the dual variables are also achieved through (7). The finite element method was then used to discretize both equations and to elaborate the numerical test described in the next section.

3 Numerical Examples

In order to extend the numerical investigations on the multiscale formulation, direct numerical simulations (DNS) were proposed and the solutions were compared with those obtained in the RVE.

Considering that this work is included in a soft biological tissues research, the geometrical and constitutive parameters are closely related to those. Considering a fibrous morphology, this study uses a model composed by two material phases: fibers and matrix.

The multiscale analysis are guided by the kinematic and pressures quantities retrieved from DNS. The multiscale boundary conditions are based on the Minimal Axial Linear Model (MALM) [2] for the displacement field and minimally constrained model for pressure field.

Considering an isotropic Neo-Hookean hyperelastic model to represent the solid skeleton behavior and the Darcy law with a isotropic constant permeability, the principal parameters used in the analysis are summarized in Table 1. Figure 1 presents the numerical model used in the DNS and multiscale analysis. In this case, three different sample location are retrieved from DNS and the results verified with the RVE. The DNS is based on a displacement-guided monotonic uniaxial test with a drained fluid condition. In this case, the displacement was prescribed in the axial direction of the fibers and it was controlled at 1 μm/s up to 1 μm in both top and bottom surfaces. To consider a drained case, free fluid flow (zero pore pressure boundary condition) was set only at the lateral external surfaces, allowing fluid mass exchanging with the external surroundings.

Aiming to study the influence of multiscale boundary conditions on the RVE fields, Fig. 2, Fig. 3 and Fig. 4 present some micro-scale fields results for three different sample location on DNS, central, lateral and diagonal, respectively. All results are depicted at the 5% instant of the macro-scale axial strain.

One can see that the displacement field and strain pattern can be adequately recovered from this multiscale analysis. This is consistent with the conclusions pointed out in the work Carniel et al. [2], which indicates that the MALM seems to be suitable for the case of fibrous RVE.

However, when the fields related to the fluid problem are observed, although the pore pressure field seems to have a reasonable good representation, the results of relative velocities show that the minimally constraint condition is inadequate to represent the DNS drained case.

This issue is directly related to boundary condition of the multiscale model. It can easily be seen that in the DNS sample there is a non-null net fluid flux, due to the drained condition. On the other hand, the minimally model on the RVE imposes an undrained condition on the RVE boundaries, leading to a null net fluid flux, being inconsistent with volume changes.

Despite the discussion of the size of the RVE not satisfying the separation of scales in transient problems, this results point out that the classical decomposition used in the microscopic fields, combined with the minimally constraint models, seems to be insufficient to represent the fluid velocities in a drained case. Therefore, it becomes necessary to propose alternatives to represent the fluid fields, which is already a new work in progress.

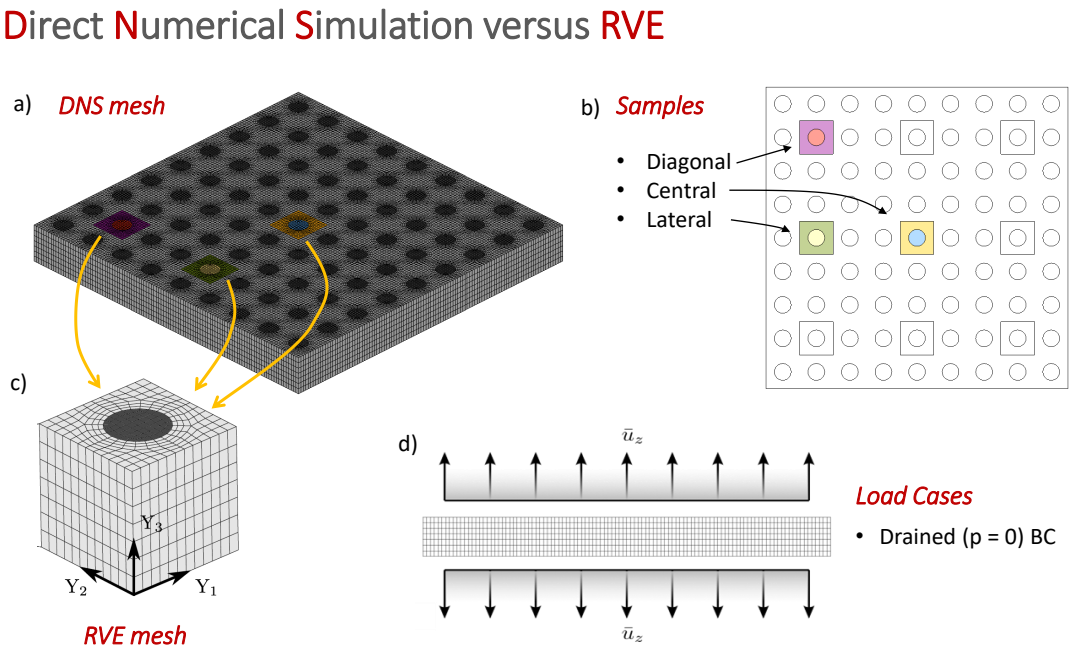

Figure 1. Representation of the geometry and the finite element mesh of the numerical specimen and RVE used in the analysis. a) Mesh of the specimen used in the DNS. b) Model with the finite element mesh used in the DNS. b) Sketch emphasizing the samples localization. c) Micro-scale model with the finite element model (Sample and RVE). d) 2D view showing the boundary conditions of the DNS in the drained case.

Table 1. Principal geometrical and constitutive parameters used in analyses.

Geometrical			Constitutive		
Parameter	**Value**	**Units**	**Parameter**	**Value**	**Units**
DNS size	90.0	μm	Fiber Lamé's first parameter	10.0	MPa
RVE size	10.0	μm	Fiber Lamé's second parameter	15.0	MPa
Fiber diameter	5.0	μm	Fiber Darcy's permeability	$1 \cdot 10^{-4}$	$\mathrm{mm}^4/\mathrm{Ns}$
Fiber volume fraction	~ 20	%	Matrix Lamé's first parameter	1.0	MPa
			Matrix Lamé's second parameter	1.5	MPa
			Matrix Darcy's permeability	$2 \cdot 10^{-4}$	$\mathrm{mm}^4/\mathrm{Ns}$

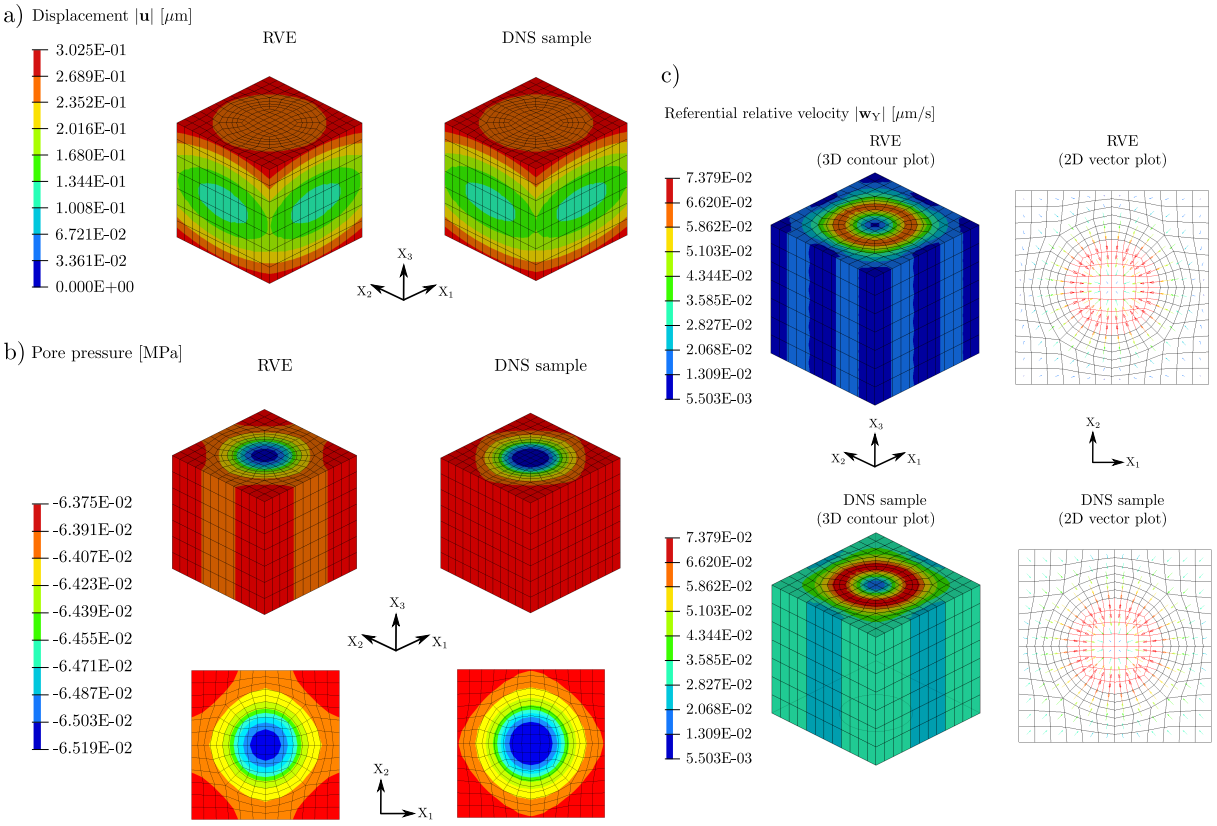

Figure 2. Comparative results RVE/DNS of the central sample at 5% of axial macroscopic strain. a) Amplitude of the displacement field $|\mathbf{u}|$. b) Pore pressure field. c) Amplitude of the referential relative velocity field $|\mathbf{w}_Y|$. The 3D contour plot and the 2D vector plot at the fiber transverse surface.

4 Conclusions

This paper aimed to discuss important points of the multiscale poromechanical theory for large deformations. Although good results were obtained for the displacement and pore pressure fields, the cases presented show that the model fails to represent the relative fluid velocity patterns due to restrictions imposed by the minimal boundary conditions. Even knowing that the chosen RVE does not satisfy the principle of scale separation for transient problems, the aspects of the boundary conditions applied to the micro-scale are discussed, mainly given fluid flux constraints applied on the boundaries of the RVE. For each of the chosen sample's location (central, lateral and diagonal), it is observed that the displacement and pressure fields consistently approximate the results obtained via DNS. However, when the pressure gradients, i.e., relative velocity fields are taken, it is seen that the fluid paths are distinct, indicating that the applied boundary conditions do not allow for a liquid fluid flow into the RVE (i.e., micro-scale shrinkage or swelling).

Acknowledgements. The authors would like to thank the following funding agencies: CAPES - (Coordination for the Improvement of Higher Education Personnel) and CNPq - (National Council for Scientific and Technological Development).

Authorship statement. The authors hereby confirm that they are the sole liable persons responsible for the authorship of this work, and that all material that has been herein included as part of the present paper is either the property (and authorship) of the authors, or has the permission of the owners to be included here.

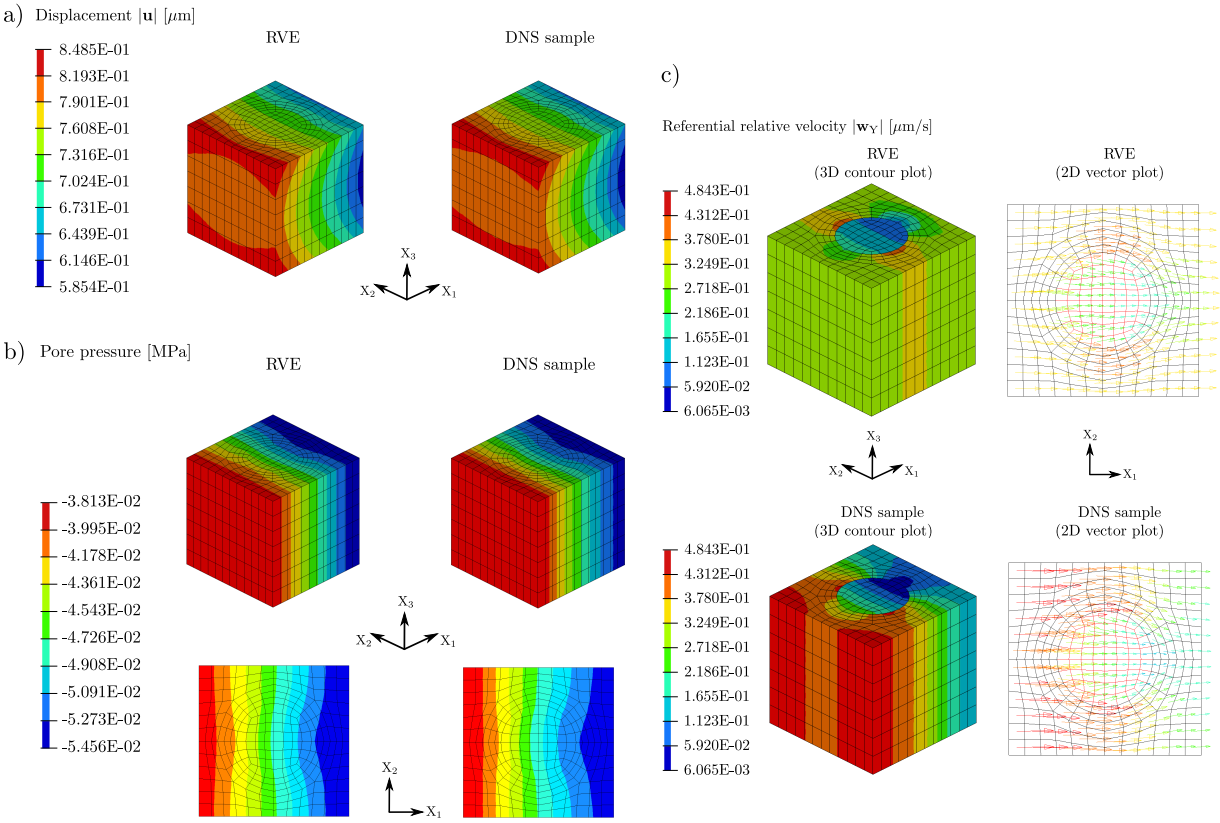

Figure 3. Comparative results RVE/DNS of the lateral sample at 5% of axial macroscopic strain. a) Amplitude of the displacement field $|\mathbf{u}|$. b) Pore pressure field. c) Amplitude of the referential relative velocity field $|\mathbf{w}_Y|$. The 3D contour plot and the 2D vector plot at the fiber transverse surface.

References

[1] N. S. Kalson, Y. Lu, S. H. Taylor, T. Starborg, D. F. Holmes, and K. E. Kadler. A structure-based extracellular matrix expansion mechanism of fibrous tissue growth. *eLife*, vol. 4, 2015.

[2] T. A. Carniel, B. Klahr, and E. A. Fancello. On multiscale boundary conditions in the computational homogenization of an RVE of tendon fascicles. *Journal of the Mechanical Behavior of Biomedical Materials*, vol. 91, pp. 131–138, 2019.

[3] F. S. Passini, P. K. Jaeger, A. S. Saab, S. Hanlon, N. A. Chittim, M. J. Arlt, K. D. Ferrari, D. Haenni, S. Caprara, M. Bollhalder, and others. Shear-stress sensing by piezo1 regulates tendon stiffness in rodents and influences jumping performance in humans. *Nature Biomedical Engineering*, vol. 5, n. 12, pp. 1457–1471, 2021.

[4] A. Waseem, T. Heuzé, L. Stainier, M. G. Geers, and V. G. Kouznetsova. Enriched continuum for multi-scale transient diffusion coupled to mechanics. *Advanced Modeling and Simulation in Engineering Sciences*, vol. 7, n. 1, pp. 1–32, 2020.

[5] A. Khoei and S. Saeedmonir. Computational homogenization of fully coupled multiphase flow in deformable porous media. *Computer Methods in Applied Mechanics and Engineering*, vol. 376, pp. 113660, 2021.

[6] R. Jänicke, F. Larsson, and K. Runesson. A poro-viscoelastic substitute model of fine-scale poroelasticity obtained from homogenization and numerical model reduction. *Computational Mechanics*, vol. 65, n. 4, pp. 1063–1083, 2020.

[7] P. J. Blanco, P. J. Sánchez, E. A. de Souza Neto, and R. A. Feijóo. Variational Foundations and Generalized Unified Theory of RVE-Based Multiscale Models. *Archives of Computational Methods in Engineering*, vol. 23, n. 2, pp. 191–253, 2016.

[8] M. Levenston, E. Frank, and A. Grodzinsky. Variationally derived 3-field finite element formulations for quasistatic poroelastic analysis of hydrated biological tissues. *Computer Methods in Applied Mechanics and Engineering*, vol. 156, n. 1-4, pp. 231–246, 1998.

[9] C. W. MacMinn, E. R. Dufresne, and J. S. Wettlaufer. Large deformations of a soft porous material. *Physical Review Applied*, vol. 5, n. 4, pp. 044020, 2016.

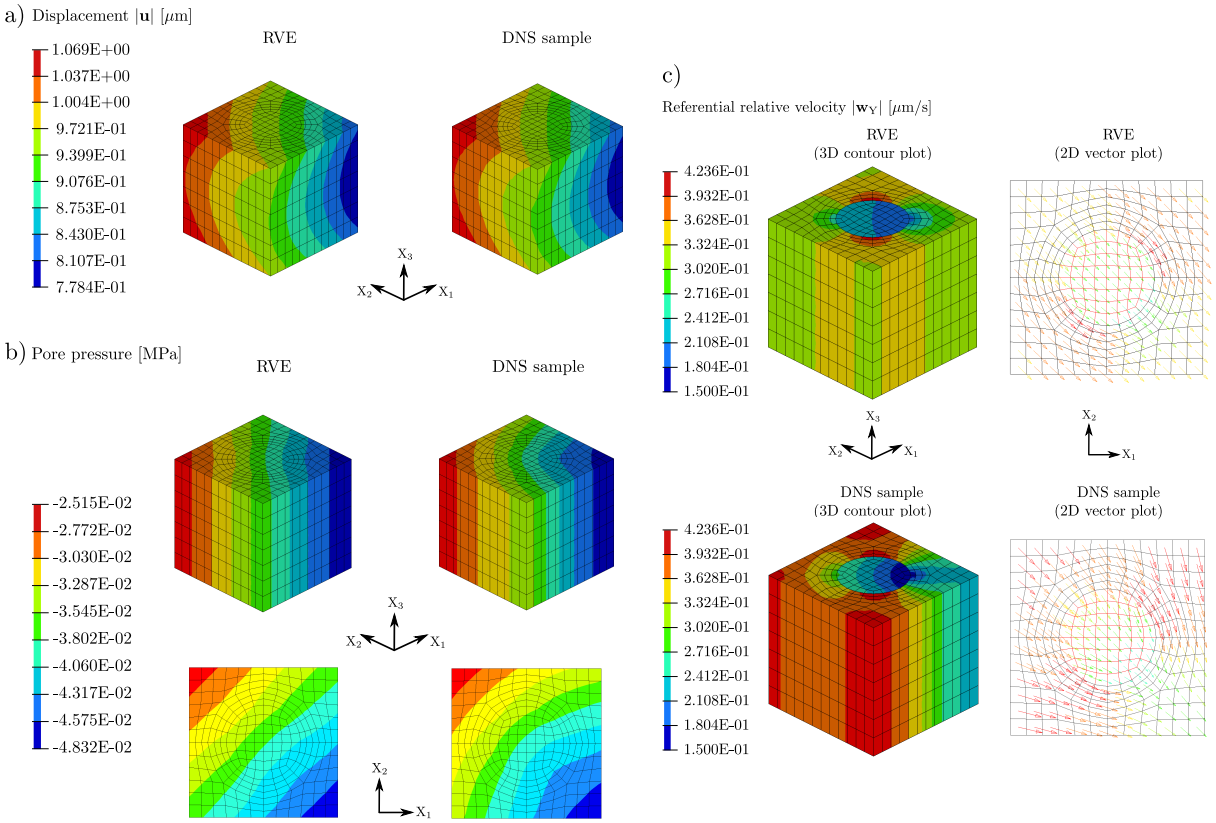

Figure 4. Comparative results RVE/DNS of the diagonal sample at 5% of axial macroscopic strain. a) Amplitude of the displacement field $|\mathbf{u}|$. b) Pore pressure field. c) Amplitude of the referential relative velocity field $|\mathbf{w}_Y|$. The 3D contour plot and the 2D vector plot at the fiber transverse surface.

[10] B. Klahr, J. L. M. Thiesen, O. T. Pinto, T. A. Carniel, and E. A. Fancello. An investigation of coupled solution algorithms for finite-strain poroviscoelasticity applied to soft biological tissues. *International Journal for Numerical Methods in Engineering*, vol. n/a, n. n/a, 2022.
[11] R. Hill. On constitutive macro-variables for heterogeneous solids at finite strain. *Proceedings of the Royal Society of London. Series A, Mathematical and Physical Sciences*, vol. 326, n. 1565, pp. 131–147, 1972.
[12] J. Mandel. Plasticité classique et viscoplasticité, lectures notes int. centre for mech. sci.(udine, 1971), 1972.